

Low-temperature resistance and its temperature dependence in nanostructured silver

X. Y. Qin, W. Zhang, L. D. Zhang, and L. D. Jiang

Institute of Solid State Physics, Academia Sinica, 230031 Hefei, China

X. J. Liu and D. Jin

Laboratory of Ultra-Low Temperature Physics, Cryogenic Laboratory, Academia Sinica, 100080 Beijing, China

(Received 21 August 1996; revised manuscript received 28 April 1997)

The dc resistance and the temperature coefficient of resistance (TCR) of bulk nanostructured silver (n -Ag), synthesized by inert gas condensation and *in situ* vacuum compaction as well as by the sol-gel method, was investigated in the temperature range from 4.2 to 300 K. The results indicated that for all of the n -Ag specimens with larger grain sizes ($d > 20$ nm) and higher densities (relative density $D > 88\%$) investigated, their resistivity decreased with decreasing temperature, showing metallic behavior; however, it was found that for the n -Ag with smaller grain sizes and lower density ($D = 45\text{--}50\%$), the resistance increased with decreasing temperature (negative TCR) as its mean size $d < 9$ nm, exhibiting nonmetallic behavior. Furthermore, it was found that generally at a certain (fixed) temperature (at 280 K, for instance), there were approximately linear relations (with negative slope) between its TCR and reciprocals of both grain size and density. In addition, the absolute magnitudes of the resistivity of n -Ag were higher than that of polycrystalline silver (poly-Ag), and increased with decreasing both grain size and density. With the model of grain boundary reflection, it was evaluated that the electron mean free path at room temperature was 44 and 33 nm for the n -Ag with grain size 38.5 and 25 nm, respectively, both of which are smaller than that of poly-Ag (51 nm). It was also evaluated that the electron transmission coefficient through boundaries decreased monotonically from 0.83 to 0.42 as n -Ag density decreased from 98.5 to 88%, suggesting greater boundary barriers in the n -Ag's with lower densities. The fact that transition of TCR sign from positive to negative can be attributed mainly to the dominant scattering caused by interfaces as compared to that caused by intragranular phonons in n -Ag with extremely fine grain sizes and low densities. [S0163-1829(97)07936-8]

I. INTRODUCTION

Nanostructured materials (n -materials) are artificial synthesized polycrystalline materials whose grain sizes are of the order of several to dozens of nanometers.¹ Since the fraction of interfacial component in n -materials is comparable to that of the intragranular component (for instance, the fraction of interfaces is $\sim 50\%$ for the n -materials with grain size 5 nm), the influence of the interfaces on the electron transport property cannot be neglected, as has been done in conventional polycrystalline material (polymaterial). Therefore, some features involving electrical conduction may appear that are closely associated with its structural characteristics.

The dc resistivity and its temperature behavior has been widely investigated in metallic glass^{2,3} and solid films,⁴⁻⁷ and some important results related to their structure have been obtained. In n -materials, however, this investigation is in its preliminary stage. Wu *et al.*⁸ investigated the ionic conductivity of n -Ca_{1-x}La_xF_{2+x} ($x = 0, 0.25$) and found that it is one to two orders higher than that of polycrystalline counterparts. The low-temperature resistivity of n -Pd was studied by Krag,^{1,9} who found that the temperature coefficient of resistivity (TCR) decreases with decreasing grain size. Recently, a negative TCR was found in bulk n -NiAl with lower densities ($D \leq 68\%$) by the present authors.¹⁰ At present, however, we are far from a full understanding of the characters and mechanism of the electron transport property in n -materials. In this paper, we report the investigations on the low-temperature resistance and TCR of nanostructured

Ag(n -Ag), laying emphasis on the effects of both grain size and specimen density on the resistance and its temperature dependence.

II. EXPERIMENT

The n -Ag used was synthesized by two methods. The specimens with higher densities ($D > 88\%$) and relative larger sizes ($d \geq 20$ nm) was prepared by inert-gas condensation and *in situ* vacuum compaction as described in Ref. 1. The raw material was 99.99% pure conventional polycrystalline Ag (poly-Ag). After the vacuum chamber was evacuated to the vacuum of 5×10^{-6} Pa, it was filled with helium gas to the pressure 0.1–0.3 kPa. Then nanoparticles were evaporated by a tungsten heater and collected in a cold finger filled with liquid nitrogen. Different heating currents were used to alter the grain size of nanoparticles obtained. After a certain amount of this nanopowder was collected, it was compacted *in situ* in high vacuum at different pressures (0.6–1.8 GPa) to alter the density of bulk n -Ag specimens. The obtained specimens were disk shaped 6 mm in diameter, and 0.2–0.5 mm thick. Although there are difficulties in controlling macroscopic density and mean grain size accurately, we did our utmost to ensure that the relative density differences among the specimens used to investigate size effects quantitatively were smaller than 3%; the size differences among those used to investigate density effects quantitatively were smaller than 6 nm.

The specimens with smaller grain sizes and lower densi-

TABLE I. List of the resistivity at 5 and 300 K for poly-Ag and *n*-Ag ($d=94-96.5\%$) of different grain sizes.

Specimen	poly-Ag	<i>n</i> -Ag (47 nm)	<i>n</i> -Ag (30 nm)	<i>n</i> -Ag (20 nm)
ρ_5 ($\mu\Omega$ cm)	0.04	0.49	1.90	2.69
ρ_{300} ($\mu\Omega$ cm)	1.64	2.47	3.98	5.02

ties ($D=45-50\%$) were synthesized by the sol-gel method.¹ The nanoparticles of silver were obtained from reaction of tannic acid ($C_{76}H_{52}O_{46}$) (purity: 99.9%) with silver nitrate solution (purity: 99.9%) at room temperature. By altering the concentration of silver nitrate solution, nanoparticles with different mean grain sizes were obtained. Bulk *n*-Ag was obtained by compacting the nanopowder with lower uniaxial pressure (~ 0.5 GPa) at room temperature.

The chemical components of the synthesized nanoparticles with different grain sizes were analyzed by x-ray-photoelectron spectroscopy (XPS) (model: VG ESCALAB MK II electron spectrometer). The results revealed that the samples contained trace oxygen and carbon; no obvious change of chemical components was observed in the specimens with different grain sizes. The crystalline structure and mean grain size (based on Scherrer method) of *n*-Ag specimens was analyzed by using x-ray diffraction on a Philip-PW1700 type x-ray diffractometer (XRD) and confirmed by transmission electron microscopy (TEM). The specimen densities were measured, based on the Archimedes principle, within an accuracy of $\pm 0.5\%$.

The measurement of dc resistance was carried out, in the temperature range from 4.2 to 300 K, by using the conventional four-probe method. The voltages were recorded by a *nanovoltmeter* (model 182, Keithley Inc.) and the temperature was controlled within an accuracy of ± 0.5 K.

III. RESULTS

A. Effects of grain size on the resistance

The resistivity of poly-Ag and *n*-Ag (relative density $D=94-96.5\%$) with different grain size was measured. Table I gives the residual resistivity at 5 K and that at 300 K for poly-Ag and *n*-Ag with different grain sizes. It shows clearly that, whether the absolute magnitude of resistivity of *n*-Ag is at 5 K or at 300 K, it is greater than the corresponding values for poly-Ag, and increases with decreasing grain size. The resistivity ratio of the resistivity at different temperatures to that at 5 K was plotted as a function of temperature in Fig. 1. Comparing with poly-Ag, some features about the resistivity of *n*-Ag can be seen from this figure: (1) Similar to poly-Ag, the resistivity of *n*-Ag decreases linearly with decreasing temperature at temperatures above ~ 40 K, showing metallic behavior. (2) The slope of the linear part ($T > 40$ K) of the curve ρ/ρ_5 versus T of poly-Ag is much greater than those of all the *n*-Ag specimens investigated, and among these *n*-Ag's, the slope decreases with decreasing grain size. Figure 2 shows the TCR [defined as $\alpha = (1/\rho)d\rho/dT$] of poly-Ag (curve *a*) and three *n*-Ag specimens (curves *b*, *c*, and *d*) as a function of temperature. The temperature depen-

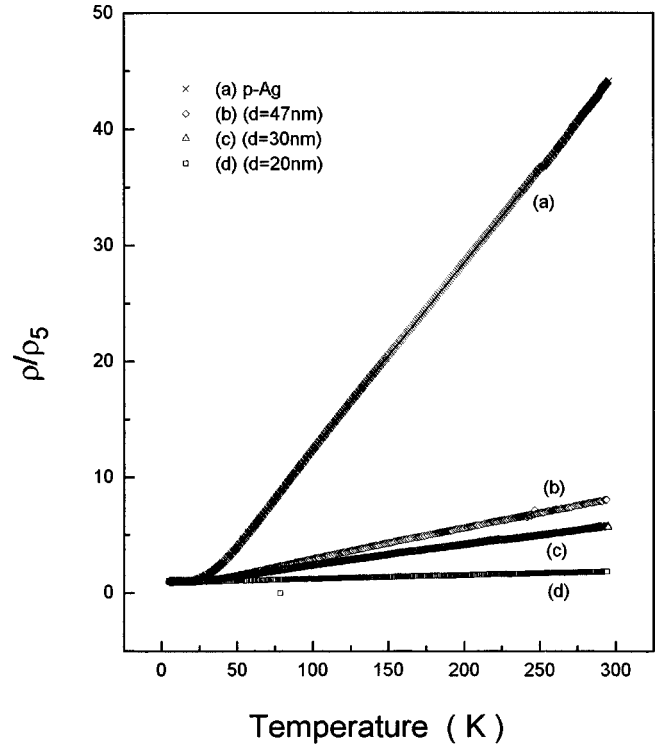


FIG. 1. Variation of resistivity ratio $\rho(T)/\rho_5$ of *p*-Ag (*a*) and *n*-Ag (*b, c, d*) with different grain sizes on temperature.

dences of TCR of *n*-Ag's with different grain sizes differ greatly from those of poly-Ag; with decreasing temperature the TCR of poly-Ag rises more rapidly than those of *n*-Ag's, indicating that the reduction of the resistance of poly-Ag is

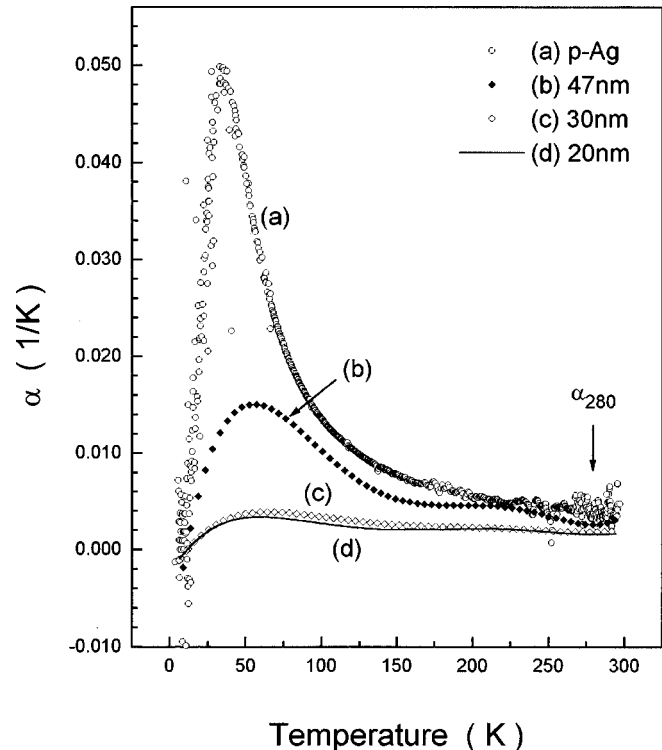


FIG. 2. Variation of TCR of poly-Ag (*a*) and *n*-Ag (*b, c, and d*) with different grain sizes on temperature.

TABLE II. List of the resistivity at 5 and 300 K for poly-Ag and *n*-Ag ($d=25\text{--}30\text{ nm}$) of different densities.

Specimen	poly-Ag	<i>n</i> -Ag ($D=98.8\%$)	<i>n</i> -Ag ($D=94.7\%$)	<i>n</i> -Ag ($D=91.7\%$)
ρ_5 ($\mu\Omega\text{ cm}$)	0.04	0.44	2.70	3.82
ρ_{300} ($\mu\Omega\text{ cm}$)	1.64	2.48	5.00	6.06

much faster than that of *n*-Ag with decreasing temperature. In addition, at a fixed temperature the TCR of *n*-Ag was much smaller than that of poly-Ag, and decreased with decreasing grain size.

B. Effects of specimen density on the resistance

Table II gives the residual resistivity at 5 K and that at 300 K for poly-Ag and *n*-Ag (grain size $d=25\text{--}30\text{ nm}$) with different densities. It can be seen that, whether the resistivity of *n*-Ag is at 5 K or at 300 K it is greater than the corresponding values for poly-Ag, and increases with decreasing density. The resistivity ratio of the resistivity at different temperatures to that at 5 K was plotted as a function of temperature in Fig. 3. It can be seen that the slope of the linear part ($T>40\text{ K}$) of the curve ρ/ρ_5 versus T of poly-Ag (whose full curve is shown in the inset) is much greater than those of all the *n*-Ag specimens investigated. Among these *n*-Ag's the slope decreases with decreasing density. Figure 4 shows the TCR of poly-Ag (curve *a*) and three *n*-Ag specimens (curves *b*, *c*, and *d*). This figure indicates that the TCR of *n*-Ag was smaller than that of poly-Ag, and decreased with decreasing density.

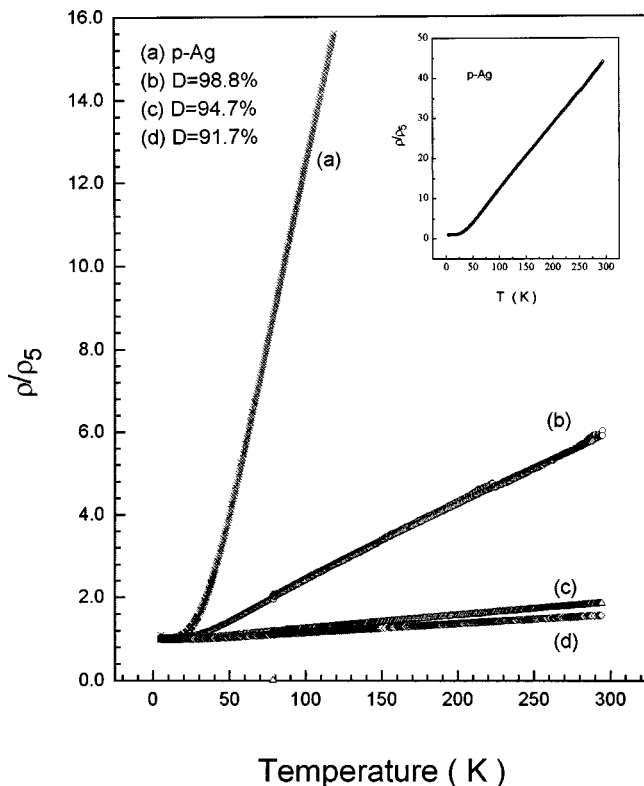


FIG. 3. Variation of resistivity ratio $\rho(T)/\rho_5$ of poly-Ag (*a*) and *n*-Ag (*b*, *c*, and *d*) with different densities on temperature. The inset shows the full curve of $\rho(T)/\rho_5$ of poly-Ag.

C. Temperature dependence of resistance of the *n*-Ag with extremely fine grain sizes and low densities

To reveal the effects of grain size and density on temperature dependence of resistance, the *n*-Ag's with smaller grain sizes and lower densities (relative density $D=45\text{--}50\%$) were synthesized and their resistance were measured in temperature range $77\text{--}300\text{ K}$. Figure 5 shows the XRD pattern of poly-Ag (*a*) and a *n*-Ag sample (*b*) (5.3 nm). It can be seen that, apart from broadening of all of the reflection peaks in curve *b* (which was mainly caused by smaller grain size), the reflection peaks in the two curves correspond to one another, indicating that the crystalline structure of the *n*-Ag sample is identical with that of poly-Ag. Moreover, no evidence of other phase, such as Ag_2O , was detected in curve *b*, which coincided with the results of XPS analysis. Figure 6 shows a typical TEM morphology of the grains of the *n*-Ag with mean grain size 6 nm determined by XRD. It can be seen that most grain sizes are around 6 nm with rather even size distribution. The inset gives the electron diffraction pattern of its structure, which is typical fcc structure—the same as that of poly-Ag.

Figure 7 gives the resistivity of these *n*-Ag's as a function of temperature. It can be seen that for *n*-Ag's with larger grain sizes ($d=11$ and 18 nm), their resistance increased

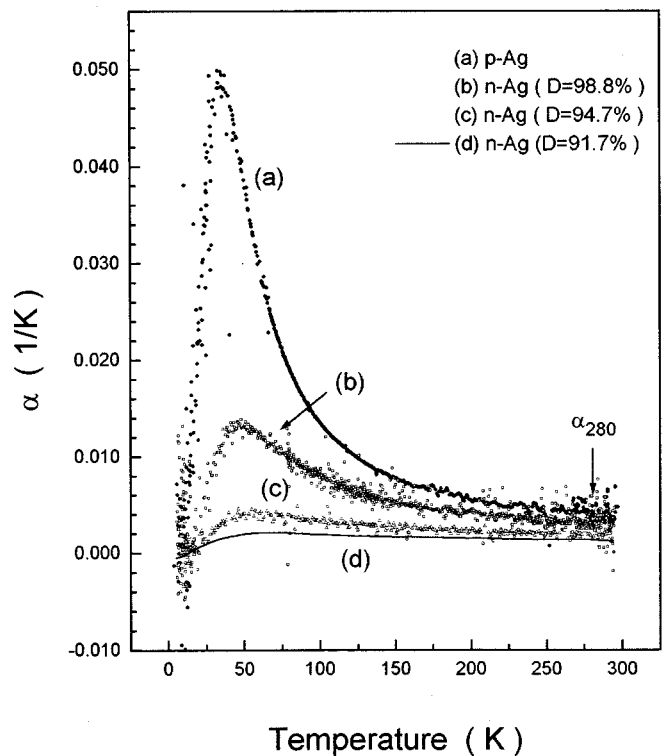


FIG. 4. Variation of TCR of poly-Ag (*a*) and *n*-Ag (*b*, *c*, and *d*) with different densities on temperature.

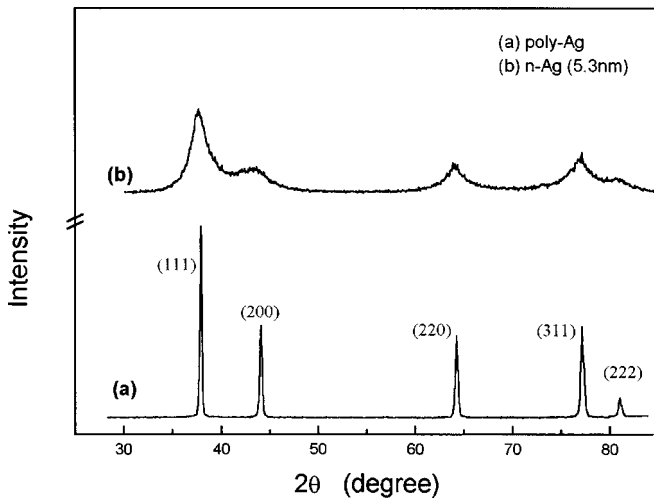


FIG. 5. X-ray-diffraction pattern of poly-Ag standard (a) and a *n*-Ag specimen (b) (mean grain size: 5.3 nm) ($\text{Cu } K\alpha$ radiation).

with increasing temperature, showing normal behavior, for the *n*-Ag specimens (having the same density as that of the specimens of larger grain sizes) with smaller mean grain sizes ($d=5.3$ and 6.8 nm); however, their resistance increased with decreasing temperature, exhibiting nonmetallic behavior, which, to our knowledge, was first observed in bulk nanostructured pure metal. In order for us to confirm the observed results and exclude possible effects produced by other factors, such as chemical purity or contamination, on the temperature behavior of resistance for the finer grain size *n*-Ag specimens, after measurement of resistance the specimen with grain size 5.3 nm was annealed at 643 K in the vacuums of 10^{-3} Pa for 2 h, and its resistance was remeasured. The result showed that as its grain size grew to 11.7 nm after annealing, its resistance decreased with decreasing temperature, showing normal behavior [see Figs. 8(a) and 8(b)]. In addition, the appearance of the nonmetallic behavior in the specimens with finer grain sizes ($d \leq 10$ nm) was of good reversibility, that is, the resistance-temperature curve measured during cooling coincided well with that measured during the heating process. To survey the transformation of

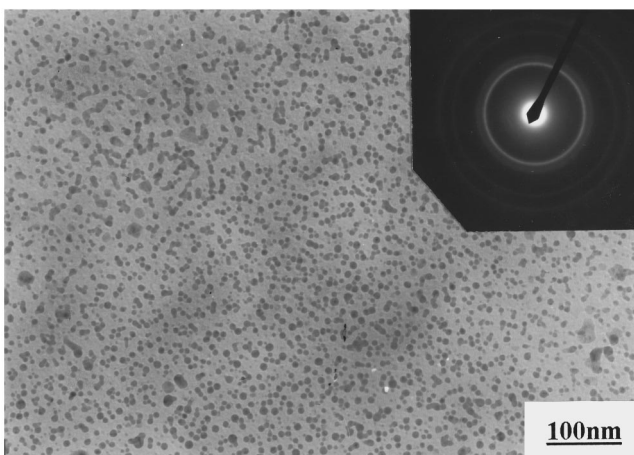


FIG. 6. The typical morphology of grains, observed by TEM, of *n*-Ag with mean grain size 6 nm. The inset shows the electron diffraction pattern of their structure.

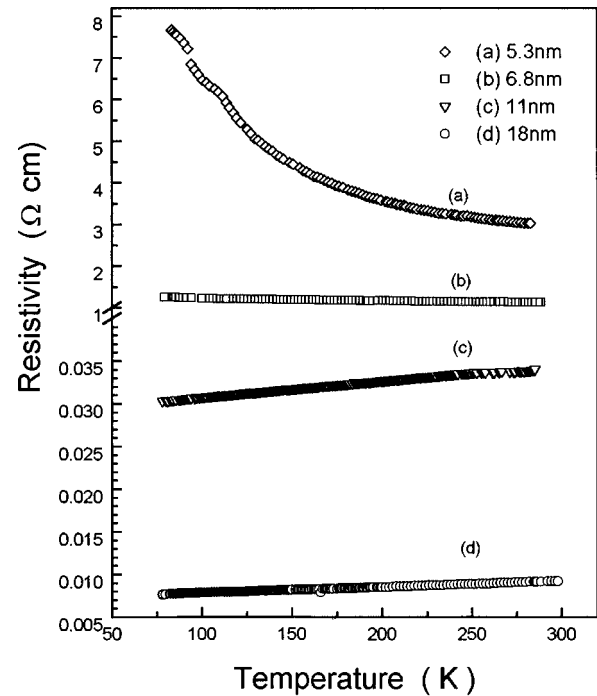


FIG. 7. Variation of the resistivities of *n*-Ag's (density $D = 45\text{--}50\%$) with different grain sizes on temperature.

its TCR from positive to negative with grain size in more detail, we investigated the dependence of TCR on its grain size of *n*-Ag, which is illustrated in Fig. 9. It can be seen clearly that with decreasing grain size the TCR whether at 100 or at 250 K, all decreased slowly with decreasing grain size; when grain size was reduced to ~ 9 nm, they changed sign from positive to negative, below which negative TCR appeared and dropped more steeply. The origin of this abnormal phenomenon will be discussed further in the following section.

IV. DISCUSSION

A. Magnitude of resistivity and microparameters of electron transport

The difference in resistivity and its temperature behavior between poly-Ag and *n*-Ag as well as among *n*-Ag's with different grain size and/or densities must be associated with the differences between their microstructure characteristics. The high resistivity of *n*-Ag as compared to that of poly-Ag (see Tables I and II) may originate from one of the following two aspects.

(a) *Macroscopic defect effects.* Since the density of *n*-Ag ($D \approx 88\text{--}99\%$) was generally lower than that of poly-Ag, there is inevitably a lot of porosity (voids with sizes of the order of $\sim 1 \mu\text{m}$); there are, as well, vacancy clusters (VC's) (with the size $d > 3$ nm) residing in triple junctions of *n*-Ag.^{11,12} Even a great number of microcracks exist in *n*-Ag, especially for those specimens with smaller densities. Their existence will lead to the reduction of effective conduction area, giving rise to extrinsic increase of its resistivity. Because the volume fractions of each type of defects, their accurate shape, their size distribution, and their spatial distribution in *n*-Ag are difficult to determine experimentally,

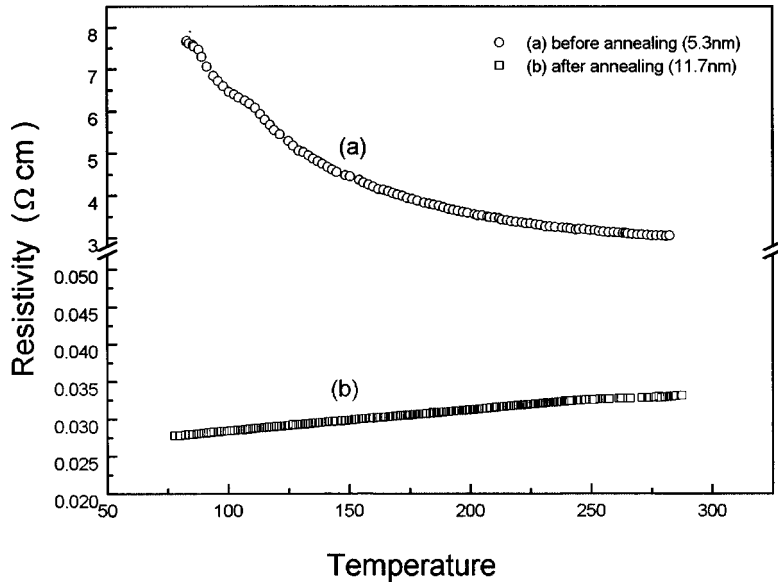


FIG. 8. The resistivity of a n -Ag specimen as a function of temperature. (a) Before annealing ($d=5.3$ nm), and (b) after annealing treatment at 643 K for 2 h ($d=11.7$ nm).

there are difficulties in quantitative deduction of the extrinsic resistivity caused by them. This should be kept in mind as we try to extract the microparameters of electron transport.

(b) *Interfacial and microscopic defect effects.* Due to the small mean grain size (20–47 nm), there is a greater number of interfaces (interfacial fraction $f \approx 6-15\%$, assuming the thickness of the grain boundary is 1 nm) in n -Ag than in poly-Ag ($f < 0.1\%$). These interfaces, which are always related to random atomic arrangements and superimposed by vacancylike (VL) defects,^{11,12} have strong scattering ability to conduction electrons and therefore cause additional resistivity. For this reason, the “intrinsic resistivity” of n -Ag is different from that of poly-Ag. The normal Drude formula $\sigma = n_0 e^2 l / m V_F$ [here m is the mass of electron, V_F the Fermi velocity, e the electron charge, n_0 the free electron density, and l the mean free path (MFP)] cannot be used to determine the microparameters, which, by using the measured intrinsic resistivity, may lead to unphysical magnitude, such as a MFP smaller than a lattice constant. The investigations on resistivity of solid state films⁵ indicated that as the grain size of polycrystalline material is comparable to the electron MFP, each crystal acts like a potential well with boundary (interface) as a barrier. As a result, a fraction of conduction electrons is localized within this well, and the effective conduction electron density is limited to those which tunnel through all the boundaries along the MFP, resulting in decrease of effective density of conduction electrons. The relationship between conductivity and microparameters is described by a modified Drude formula, and has the form^{6,7}

$$\sigma = [(e^2 l / m v_F)] n_0 G(l, d, T^*). \quad (1)$$

Here d the grain size, T^* (< 1) is the transmission coefficient of the electron through a boundary, and $G(l, d, T^*)$ gives the correction of conduction electron density due to grain boundary scattering. Using the transfer matrix approach, Reiss *et al.*¹³ calculated the function G , which in the first approximation has the form

$$G(l, d, T^*) = T^{*l/d}. \quad (2)$$

or

$$n \equiv n_0 G(l, d, T^*) = n_0 T^{*l/d}. \quad (2')$$

From formula (2') one knows that n approaches n_0 for conventional polycrystalline material ($d > 1000$ nm, $l = 20-50$ nm), where $l/d < 2 \times 10^{-2} - 5 \times 10^{-2} \ll 1$, which means that the influence of grain-boundary scattering on conduction-electron density can be neglected. In n -materials, however, the grain size is comparable to the MFP. Then the reduction of n caused by factor $T^{*l/d}$ cannot be neglected. Combining formulas (1) and (2), we have

$$\rho = [m v_F / n_0 e^2 l] T^{*-l/d}. \quad (3)$$

Here ρ is the intrinsic resistivity of n -Ag. We know from formula (3) that MFP l cannot be determined by using a

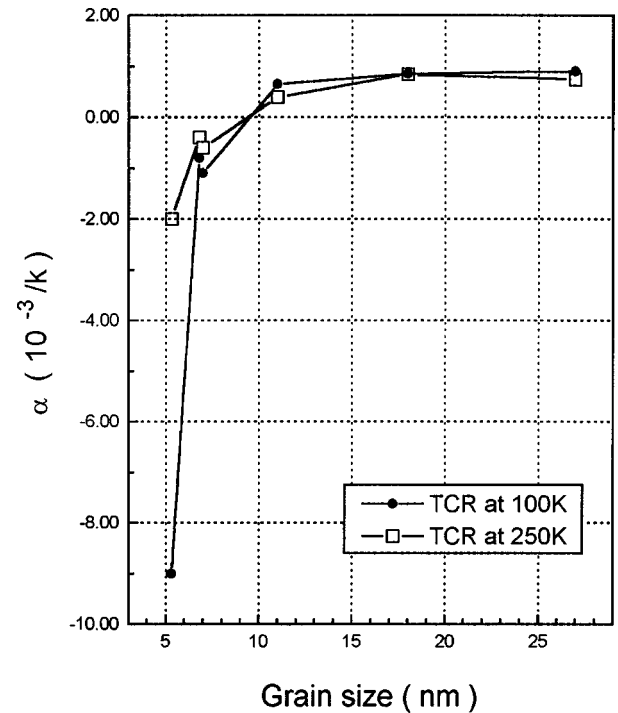


FIG. 9. Variation of TCR at 100 K (●) and at 250 K (□) of n -Ag (of lower density) on its mean grain size.

single measured ρ because there is another unknown parameter T^* in it. Since the electron transmission coefficient T^* reflects the energy barriers of grain boundaries, the determination of it is beneficial to understanding the interfacial structures of n -Ag. Here we evaluate the electron MFP and transmission coefficient of n -Ag based on the following three assumptions.

(i) For the n -Ag specimens with extremely high densities, for instance $D > 98\%$, the influence of macroscopic defects on resistivity of n -Ag can be neglected, i.e., extrinsic resistivity caused by these defects can be neglected as compared to that caused by boundaries scattering. (ii) For the specimens with identical or similar densities (for instance $\Delta D < 2\%$), their transmission coefficient T^* is identical or similar. This assumption is based on the results of positron lifetime spectrum (PLS) investigations,¹¹ which showed that density is a comprehensive index reflecting the states of interfacial defects and interface formation. (iii) The MFP is a gradually changing function of grain size. This assumption is based on the results of investigations on the resistivity of solid films,¹⁴ which showed that the MFP is mainly determined by background scattering within grains, i.e., by the deviation of atomic arrangements from periodicity within grains.

Then for poly-Ag [here $G(l, d, T^*) = 1$], we have

$$\rho_P = mV_F/n_0e^2l_0 = A/l_0 \quad (4)$$

with $A = mV_F/n_0e^2$. Here l_0 is the MFP in poly-Ag. For the two n -Ag specimens with similar densities, from formula (3) we have [using assumption (ii)]

$$\rho_1 = \frac{A}{l_1} T^{*(-l_1/d_1)}, \quad (5)$$

$$\rho_2 = \frac{A}{l_2} T^{*(-l_2/d_2)}. \quad (6)$$

Here indexes 1 and 2 denote specimens 1 and 2, respectively. On obtaining formulas (5) and (6), we have considered that (in the first approximation) the effective mass of electrons and Fermi velocity in n -Ag are same as those in poly-Ag. In addition, since MFP is a gradually changing function of grain size [assumption (iii)], we can divide the specimens of different grain sizes into several sections according to their grain size, so that in each section the grain size difference of two specimens was smaller than 10 nm. Then the difference between the MFP's of the two specimens was small, and, as approximation treatment, they were replaced by a mean value, i.e., $l_1 \approx l_2 = \bar{l}$, and from formulas (5) and (6) we obtain

$$\bar{l} = \exp \left[\ln \frac{A}{\rho_1} - \frac{d_2}{d_1 - d_2} \ln \frac{\rho_1}{\rho_2} \right]. \quad (7)$$

In the same way, from formulas (5) and (6) we obtain

$$T^* = \exp \left[\frac{d_1 d_2}{\bar{l}(d_1 - d_2)} \ln \frac{\rho_1}{\rho_2} \right]. \quad (8)$$

Consequently, by using literature values¹⁵ (at 300 K) of $n_0 = 5.85 \times 10^{22}/\text{cm}^3$, $V_F = 1.39 \times 10^8$ cm/s,

TABLE III. List of evaluated mean free path (l) (at 300 K) and grain size (d) of n -Ag and poly-Ag.

Specimen	Poly-Ag	n -Ag	n -Ag
d (nm)	> 1000	38.5	25
l (nm)	51 ± 1	44 ± 4	33 ± 3

$m = 9.1 \times 10^{-31}$ kg, and $e = 1.602 \times 10^{-19}$ C, and by using experimental resistivity data available for poly-Ag and n -Ag, we obtained the MFP and transmission coefficient for poly-Ag and n -Ag, which are given in Table III and Fig. 10, respectively. It can be seen from Table III that the MFP in n -Ag is smaller than that in poly-Ag, and decreases with decreasing grain size. It is worth noticing that the MFP in n -Ag are greater than the corresponding grain size constituting the material. This fact suggests that the MFP is not directly determined by grain size, which agrees with the results of other investigations.¹⁴ The decrease of MFP with decreasing grain size mainly originated from the enhanced distortions in smaller grains, for x-ray-diffraction investigations¹⁶ showed that the lattice microstrain in smaller nanograins was generally a little larger than that in larger nanograins.

Figure 10 illustrated that with decreasing density from 99% to 88% the transmission coefficient decreases monotonically from 0.83 to 0.42. This result indicates that with decreasing density, the interfacial barriers become greater and greater, that is, the amount of interfacial defects and the random degree in grain boundaries increase with decreasing density, which agrees with the results of PLS investigations.¹¹ Figure 11 gives the plot of $\ln T^*$ versus the reciprocal of the density. The straight line is the fit to experimental data. It can be seen that a good proportional relation between $\ln T^*$ and $1/D$ exists. Its implication will be discussed in the following section.

B. Grain size and density effects on resistivity

As mentioned above, the conduction process of electrons in n -materials can be described by a modified Drude formula [see formula (3)] within which factor $T^{*-l/d}$ gives the cor-

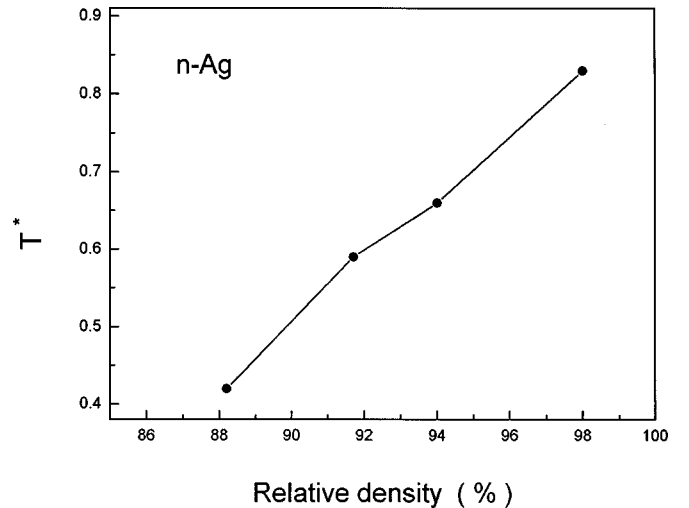


FIG. 10. Variation of transmission coefficient (at room temperature) of n -Ag on its density.

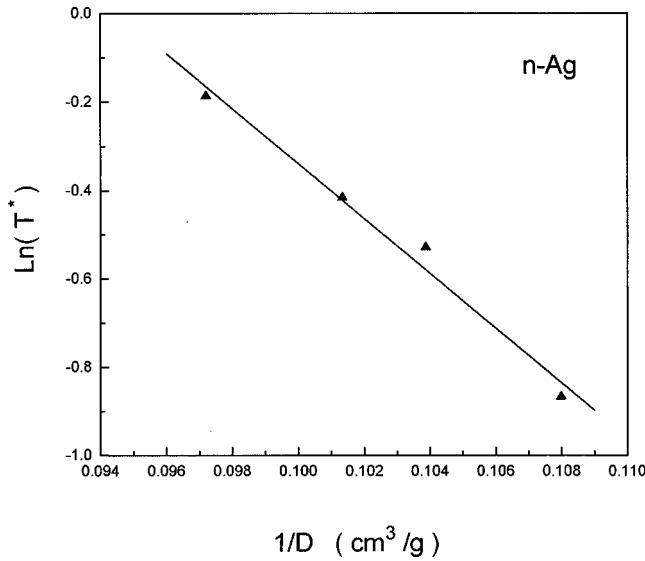


FIG. 11. Variation of transmission coefficient ($\ln T^*$) of n -Ag on reciprocal of its density. The solid straight line is the fit to evaluated values from experimental data (\blacktriangle).

rection of the conduction-electron density. With decreasing grain size, the number of interfaces (boundaries) in n -Ag increases, with its volume fraction being related to grain size by the relation of $f \approx 3\Delta/d$ (here f is the volume fraction of interfaces and Δ the thickness of grain boundaries).¹⁷ This results in intensification of electron scattering in n -Ag (which is reflected by the increase of factor l/d in $T^{*-1/d}$), leading to an increase of its resistivity. In fact, by using relation $f \approx 3\Delta/d$, from formula (3) one has $\rho = (mv_F/n_0e^2l)T^{*-(f/3\Delta)}$, which shows explicitly the relation between resistivity and number of interfaces. In addition, smaller nanograin sizes are often accompanied by greater lattice distortions,¹⁶ which leads to reduction of the MFP (see Table III). This also causes the resistivity to increase. However, the MFP influence on resistivity is relatively weaker because of the “counteracting effect.” That is, on one hand, reduction of the MFP will give rise to increase of intragranular resistance. On the other hand, however, its reduction will lead to a decrease of the number of interfaces along one MFP, resulting in an increase of effective electron density and therefore a decrease of its resistivity [see formulas (2') and (3)].

The density influence on resistivity can be divided into two aspects. (a) *Macroscopic defect effects.* As mentioned above, the existence of these defects, such as porosity or VC defects, will give rise to extrinsic resistance. Obviously, the amount of these defects will increase as density decreases,^{11,12} leading to an increase of total resistance of n -Ag. In the high-density range, their influence can be neglected. In relatively lower densities (such as $D < 90\%$), however, their influence will become important gradually. Although we cannot experimentally separate it from total resistivity accurately, the microparameters obtained here (Table III and Fig. 10) are reliable for the following reasons: (i) the densities of n -Ag specimens investigated here were generally greater than 90% (apart from one specimen with the density of 88%); (ii) the influence of extrinsic resistivity were removed to a considerable degree on obtaining the pa-

rameters because of the existence of the term $\ln(\rho_1/\rho_2)$ [see formulas (7) and (8)] (as $\rho_1/\rho_2 \approx \rho_{1i}/\rho_{2i}$, here ρ_{1i} and ρ_{2i} denote intrinsic resistivity of specimens 1 and 2, respectively). (b) *Influences of interfacial barriers.* High resolution electron microscopy (HREM) (Ref. 18) and PLS (Ref. 11) investigations showed that grain boundaries in n -materials often existed in the form of “extended states,” i.e., they are always related to random atomic arrangements and contains VL interfacial defects. Obviously, this kind of nonequilibrium interface has stronger scattering capacity to conduction electrons than normal equilibrium boundaries have. Experiments^{11,12} showed that with decreasing density the amount of VL defects increased. It can be conceivable that the interfaces containing more VL defects will have stronger scattering ability than the one with fewer VL defects. This would be manifested by the decrease of the electron transmission coefficient with decreasing density as present experiments shown in Fig. 10. Obviously, as transmission coefficient decrease, the resistivity increases [see formula (3)], which contributes partly to the variation of resistivity of n -Ag on density (see Table II).

C. Grain size and density effects on the temperature dependence of resistivity

As mentioned above, there are (other than grain boundaries) three types of defects in n -materials, i.e., porosity and VC and VL defects.^{11,12} Among them, porosity only affects the absolute value of resistance and residual resistivity due to its macroscopic character; i.e., it does not influence the TCR of n -Ag. So do the VC defects, for VC defects reside mainly in triple junctions and are also of macroscopic character due to their greater scale (10–15 monovacancies¹¹). On the other hand, in n -materials the interfaces combining with VL defects (having small T^*) and possessing great volume fraction (large f) have strong scattering capacity. Therefore the resistivity temperature behavior of n -materials is controlled by both phonon scattering within nanograins and interfacial scattering. As the temperature decreases, the MFP increases, which indicates that the resistivity caused by background scattering within grains decreases. On the other hand, however, the increase of the MFP will lead to a further descent of effective electron density [see formula (2)] because the number of grain boundaries encountered by conduction electrons along one MFP increases. In addition, as temperature decreases, thermal activation declines, which leads to descent of electron transmission coefficient T^* . All these will give rise to additional resistivity caused by boundary scattering. This would explain why the decrease of resistivity of n -Ag with decreasing temperature become slow, i.e., the increase of TCR of n -Ag with decreasing temperature becomes slower than that of poly-Ag (see Figs. 2 and 4).

According to the definition used here,

$$\alpha \equiv (1/\rho)d\rho/dT = -(1/\sigma)d\sigma/dT. \quad (9)$$

Substituting formulas (1) and (2) into (9), one obtains

$$\alpha = -[(1/l) + (1/d)\ln T^*] \frac{\partial l}{\partial T}. \quad (10)$$

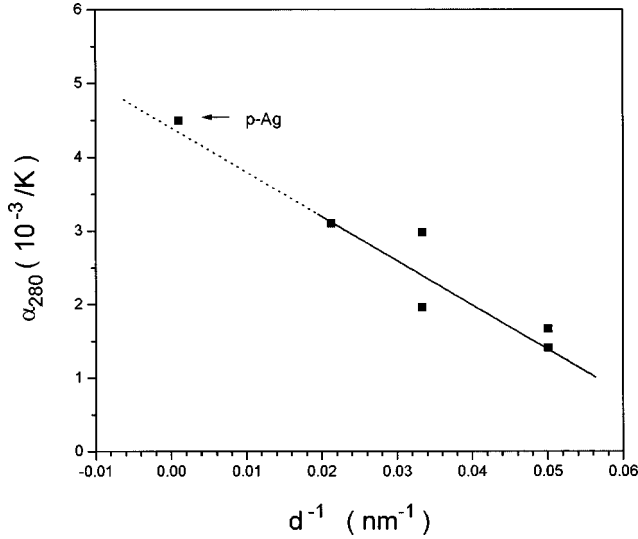


FIG. 12. Variation of TCR at 280 K (α_{280}) on reciprocal of grain size. The solid straight line is the fit to the experimental data (■).

In high temperatures $T > 0.5\Theta_D$ [here Θ_D (~ 225 K) is the Debye temperature of silver], there is a relation $1/l \propto T$, and therefore

$$\frac{\partial l}{\partial T} = -Bl^2. \quad (11)$$

Here $B(>0)$ is a constant related to the material. Substituting Eq. (11) into formula (10), one has

$$\alpha = Bl[1 - (1/d)l \ln(1/T^*)]. \quad (12)$$

Formula (12) indicates qualitatively that as grain size decreases ($1/d$ increases), the TCR decreases as seen in Fig. 2. In addition, it also indicates that as grain size $d \rightarrow \infty$ (the case in conventional polymaterials) $\alpha \rightarrow Bl$, which is the TCR of polymaterial. Hence if one plots the TCR (at a temperature) versus the reciprocal of grain size of n -Ag, he will obtain a straight line with negative slope and by extrapolating l/d to zero, it passes through the TCR of poly-Ag. Figure 12 shows the plot of α_{280} (the TCR at 280 K) versus $1/d$. It can be seen that a straight line exists indeed, and within the scope of experimental error it pass through the α_{280} of poly-Ag.

As mentioned above, the resistivity temperature behavior of n -materials is controlled by both phonon scattering within nanograins and interfacial scattering, and the interfacial scattering enhances with decreasing temperature. Obviously, as the interfacial scattering becomes dominant, then the total resistance of the n -materials will possibly increases with decreasing temperature, showing nonmetallic behavior. It can be known from formula (12) that the requirement for this transformation of the TCR from positive to negative can be realized as the term in the bracket of formula (12) is smaller than zero, that is, as the condition

$$(1/d)\ln(1/T^*) > 1 \quad (13)$$

or

$$T^* < \exp(-d/l) \quad (13')$$

is satisfied, the TCR becomes negative. Formula (13') indicates that $\exp(-d/l)$ decreases rapidly with increasing grain size. For conventional polymaterial ($d > 1000$ nm, $l = 20-50$ nm) where $d/l > 0.5 \times 10^2 - 5 \times 10^2 \gg 1$, $\exp(-d/l) \rightarrow 0$, while their $T^* \rightarrow 1$. Hence, formula (13') usually cannot be satisfied there, which explains why few negative temperature coefficients of resistance appear in normal metals. Clearly, for a given n -material, only those specimens with smaller grain sizes d and smaller densities [T^* decreases with decreasing density (see Fig. 10), or, increasing height or/and width of boundary barrier¹⁹] can possibly satisfy formula (13'). Hence, it is understandable that a negative TCR only appeared in the specimens with both extremely fine grain size and low density as observed in n -Ag's by the present authors (see Figs. 7-9).

For the case of high boundary barrier (as in n -materials) and weak field, the transmission coefficient T^* , according to quantum mechanics theory, is the tunneling probability of an electron through a boundary barrier, and has the relation¹⁹

$$T^* \approx \exp(-2\beta W) \quad (14)$$

with

$$\beta = \sqrt{(2m/\hbar)(U-E)}.$$

Here W is the width of the boundary barrier, U the height of the barrier, E the kinetic energy of electrons, and \hbar the Planck constant. In the case of high boundary barrier and weak field, the relation $E/U \ll 1$ holds approximately. Hence

$$\beta = \sqrt{(2m/\hbar)(U-E)} \approx U^{1/2}(2m/\hbar)^{1/2}.$$

Consequently one has the relation [see formula (14)]

$$\ln T^* = (-2\beta W) \approx -aWU^{1/2} \quad (15)$$

with $a [= 2(2m/\hbar)^{1/2} > 0]$ being a constant. Roughly speaking, the macroscopic density of n -materials is a parameter which reflects, to a certain degree, the coupling state among grains, and we assumes that in a certain density range, for instance in the relative density 88-99 %, the density is related to the grain boundary barrier by the following relation:

$$D \propto (WU^{1/2})^{-1} \text{ or } 1/D \propto (WU^{1/2}). \quad (16)$$

The assumption of the relation $1/D \propto (WU^{1/2})$ actually assumes that $-\ln T^*$ is proportional to $1/D$ [see formula (15)]. While this proportional relation between $-\ln T^*$ and $1/D$ has been verified by experiments as illustrated in Fig. 11. By substituting formulas (15) and (16) into (12), we obtain the relation

$$\alpha = Bl \left[(1+C) - \frac{1}{D} \left(\frac{al}{bd} \right) \right]. \quad (17)$$

Here, $b(>0)$ and C are constant. Formula (17) indicates qualitatively that at a certain (fixed) temperature, there is a linear relation between $1/D$ and the TCR (with a negative slope) for an n -material. Figure 13 plotted the TCR at 280 K as a function of reciprocal of density of n -Ag. It can be seen that approximately a linear relation between α_{280} and $1/D$ exists indeed, which also implies that the assumed condition $U > E$ holds for n -Ag in present experiments. It is worthwhile to point out that because the slope of the straight

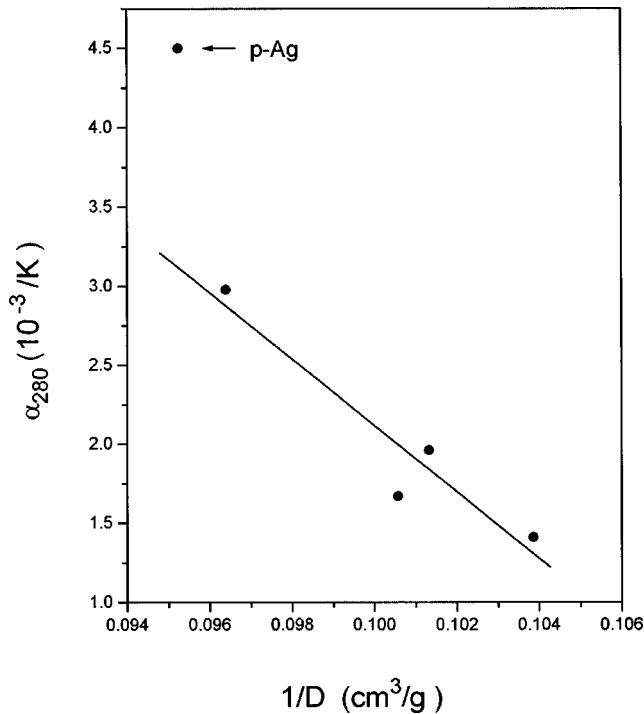


FIG. 13. The plot of TCR at 280 K vs reciprocal of density ($1/D$) of n -Ag. The solid straight line is the fit to the experimental data (●).

line is inversely proportional to grain size d [see formula (17)], it is usually about three orders greater in n -materials ($d \sim 1$ nm) than in corresponding polymaterials ($d \sim 1 \mu\text{m}$). Hence, the fact that obvious changes of the TCR with density can only be observed in n -materials is reasonable.

V. SUMMARY AND CONCLUSIONS

The dc resistivity and its temperature dependence was experimentally investigated and following conclusions can be drawn.

(1) For all the n -Ag specimens with larger grain sizes ($d > 20$ nm) and higher densities ($D > 88\%$) investigated, their resistivity decreased with decreasing temperature, showing metallic behavior. For the n -Ag with smaller grain sizes and lower density ($D = 45\text{--}50\%$), however, its resistance increased with decreasing temperature as its grain size $d < 9$ nm, exhibiting nonmetallic behavior. Generally, linear relations between the TCR at a (fixed) temperature and reciprocals of both grain size and density existed, which can be interpreted well based on an interfacial reflection model.

(2) All their magnitudes of n -Ag's with different sizes and density were higher than that of poly-Ag at corresponding temperatures, and increased with decreasing both grain size and density. In addition to the extrinsic resistivity caused by macroscopic defects, this high resistivity of n -Ag's can be attributed to intense scattering by interfaces and interfacial defects. With the model of grain boundary reflection, it was evaluated that the electron MFP at room temperature was 44 and 33 nm for the n -Ag with grain sizes 38.5 and 25 nm, respectively, both of which are smaller than that of poly-Ag (51 nm). It was also evaluated that the electron transmission coefficient decreased monotonically from 0.83 to 0.42 as n -Ag density decreased from 98.5 to 88%, suggesting greater grain-boundary barriers in the n -Ag's with lower densities.

ACKNOWLEDGMENTS

The authors thank Dr. Y. P. Sun and Professor J. J. Du for rendering great help in the measurements of resistance.

- ¹H. Gleiter, *Prog. Mater. Sci.* **33**, 223 (1989).
- ²J. H. Mooij, *Phys. Status Solidi A* **17**, 521 (1973).
- ³P. J. Cote, L. V. Meisel, in *Glassy Metals, Vol. I*, edited by H. J. Güntherodt and H. Beck (Springer, Berlin, 1981), p. 141.
- ⁴G. Fischer, H. Hoffmann, and J. Vancea, *Phys. Rev. B* **22**, 6065 (1980).
- ⁵J. Vancea and H. Hoffmann, *Thin Solid Films* **92**, 219 (1982).
- ⁶J. Vancea, H. Hoffmann, and K. Kastner, *Thin Solid Films* **121**, 201 (1984).
- ⁷J. Vancea, S. Pukowitz, G. Reiss, and H. Hoffmann, *Phys. Rev. B* **35**, 9067 (1987).
- ⁸X. J. Wu, F. Su, X. Y. Qin, B. Xie, and X. L. Ji, in *Nanophase and Nanocomposite Materials*, edited by S. Komaneri, J. C. Parker, and G. J. Thomas, MRS Symposia Proceedings No. 286 (Materials Research Society, Pittsburgh, 1993), p. 27.
- ⁹P. Krag, Diploma thesis, University of the Saarland, Saarbrücken, Germany FB, Series No. 21.1 (1990).
- ¹⁰X. Y. Qin, L. D. Zhang, B. M. Wu, M. L. Tian, Y. L. Du, D. S. Yang, and L. Z. Cao, *J. Appl. Phys.* **80**, 4776 (1996).
- ¹¹H. E. Schaefer, R. Würschum, R. Birringer, and H. Gleiter, *Phys. Rev. B* **38**, 9545 (1988).
- ¹²X. Y. Qin, J. S. Zhu, X. Y. Zhou, and X. J. Wu, *Phys. Lett. A* **193**, 335 (1994).
- ¹³G. Reiss, J. Vancea, and H. Hoffmann, *Phys. Rev. Lett.* **56**, 2100 (1986).
- ¹⁴J. Vancea, G. Reiss, and H. Hoffmann, *Phys. Rev. B* **35**, 6435 (1987).
- ¹⁵C. Kittel, *Introduction to Solid State Physics*, 5th ed. (Wiley, New York, 1976), pp. 154 and 610.
- ¹⁶G. W. Nieman, J. R. Weertman, and R. W. Siegel, *J. Mater. Res.* **6**, 1012 (1991).
- ¹⁷T. Mutschele and R. Kirchheim, *Scr. Metall.* **21**, 1101 (1987).
- ¹⁸Wunderlich, Y. Ishida, and R. Maurer, *Scr. Metall. Mater.* **24**, 403 (1990).
- ¹⁹F. Warkusz, *Thin Solid Films* **161**, 1 (1988).